Classification of Leukemia Blood Samples Using Neural Networks

Article *in* Annals of Biomedical Engineering · December 2009

DOI: 10.1007/s10439-009-9866-z · Source: PubMed

6 authors, including:

Malek Adjouadi
Florida International University
327 PUBLICATIONS **2,416** CITATIONS

SEE PROFILE

Annals of Biomedical Engineering, Vol. 38, No. 4, April 2010 (© 2009) pp. 1473–1482
DOI: 10.1007/s10439-009-9866-z

Classification of Leukemia Blood Samples Using Neural Networks

MALEK ADJOUADI, MELVIN AYALA, MERCEDES CABRERIZO, NUANNUAN ZONG, GABRIEL LIZARRAGA, and MARK ROSSMAN

Department of Electrical & Computer, Center for Advanced Technology and Education, Florida International University, 10555 W. Flagler Street, EAS 2672, Miami, FL 33174, USA

(*Received 2 October 2009; accepted 2 December 2009; published online 15 December 2009*)

Associate Editor Scott I. Simon oversaw the review of this article.

Abstract—Pattern recognition applied to blood samples for diagnosing leukemia remains an extremely difficult task which frequently leads to misclassification errors due in large part to the inherent problem of data overlap. A novel artificial neural network (ANN) algorithm is proposed for optimizing the classification of multidimensional data, focusing on acute leukemia samples. The programming tool established around the ANN architecture focuses on the classification of normal vs. abnormal blood samples, namely acute lymphocytic leukemia (*ALL*) and acute myeloid leukemia (*AML*). There were 220 blood samples considered with 60 abnormal samples and 160 normal samples. The algorithm produced very high sensitivity results that improved up to 96.67% in *ALL* classification with increased data set size. With this type of accuracy, this programming tool provides information to medical doctors in the form of diagnostic references for the specific disease states that are considered for this study. The results obtained prove that a neural network classifier can perform remarkably well for this type of flow-cytometry data. Even more significant is the fact that experimental evaluations in the testing phase reveal that as the *ALL* data considered is gradually increased from small to large data sets, the more accurate are the classification results.

Keywords—Blood cell classification, Leukemia diagnosis, Acute lymphocytic leukemia, Acute myeloid leukemia, Artificial neural networks.

INTRODUCTION

Normal white blood cells (WBC) include lymphocytes, neutrophils, eosinophils, basophils, and monocytes that are produced by bone marrow to help the body fight infection and other diseases. Abnormal white blood cells include blasts, immature granulocytes, and atypical lymphocytes. One method of determining that a medical abnormality may exist in the blood of a patient is to note when the subpopulations exceed the acceptable normal white blood cell population. The presence of unhealthy white blood cells leads to a host of complications such as deficiency of the immune system, coagulation problems, swollen lymph nodes, and other adverse medical conditions. A normal blood cell subpopulation map is *a priori* established as a standard platform based on statistical analysis of patients' flow-cytometry data. This model is often regarded as an "average case", representing the expected locations and types of blood cells that will appear whenever a blood sample is analyzed by a flow cytometer and displayed as a dot plot with the dimensional parameters of absorbance and volume. In this common and well-established model,[8] normal cell types and their locations are as shown in Fig. 1.

Acute leukemia is a type of cancer in which the bone marrow makes immature white blood cells that do not develop and cannot fight infections. When it affects lymphoid cells, it is called lymphocytic leukemia, but when myeloid cells are affected, the disease is called myeloid leukemia. These two types of leukemia are in general characterized by an accumulation of abnormal lymphocytes in blood and bone marrow. This departure from the normal distribution of white blood cells may be used as an initial indicator for the disease.[32]

Typically, leukemia can be diagnosed by an abnormal result on a complete blood count. It has been also a practice in cytometry to use fluorescence for the diagnosis of this disease.[11,23,24] This study will prove that it is possible to look at other cytometry parameters to classify blood samples in two categories (normal and abnormal) by using artificial neural networks (ANNs).

It is not the intention of this study to explore the nature of flow-cytometry data and its acquisition. Rather, the attention will be focused to the mathematical manipulation of this data and the creation of an algorithm for blood sample classification.

Address correspondence to Mercedes Cabrerizo, Department of Electrical & Computer, Center for Advanced Technology and Education, Florida International University, 10555 W. Flagler Street, EAS 2672, Miami, FL 33174, USA. Electronic mail: adjouadi@fiu.edu, cabreriz@fiu.edu

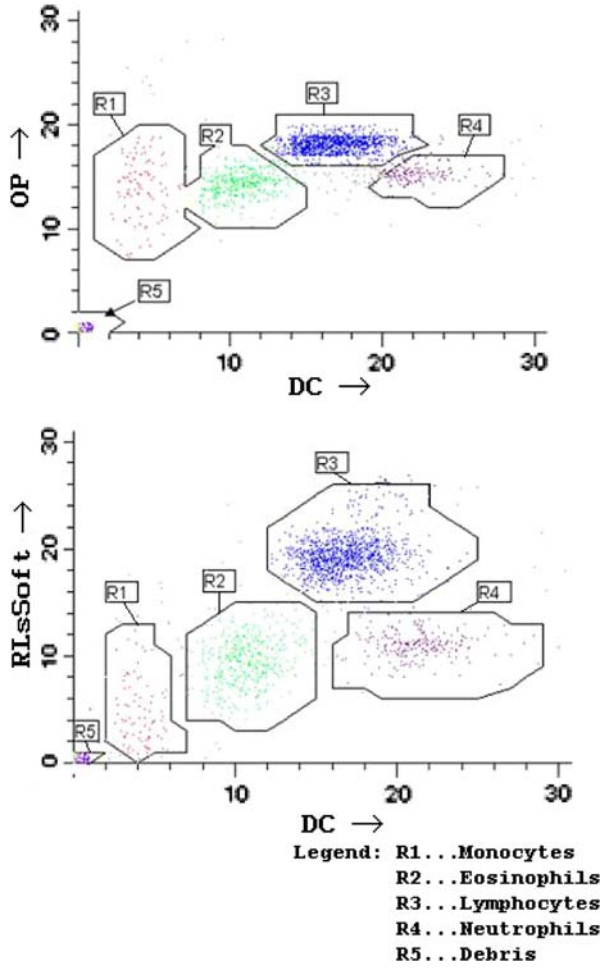

FIGURE 1. Illustrative examples of normal blood samples using dot-plot displays. Note the separation between the data clusters.

MATERIALS AND METHODS

Description of the Problem

As a practical implementation case, this study considered data samples with acute lymphocytic leukemia and acute myeloid leukemia, common diseases with thousands of new cases found yearly in the US alone. An acute leukemia patient's marrow makes too many blast cells (immature white blood cells). These blast cells should normally mature into healthy white blood cells (such as lymphocytes, neutrophils, monocytes… etc.), but they do not. So many blast cells appear that the marrow no longer has the ability to produce suitable quantities of normal red blood cells, white blood cells, and platelets. According to the information available on leukocyte subpopulations, it is necessary to analyze the physical characteristics associated with their parametric representation.[5] Because of the extremely large number of blood cells that exist in a given sample, compounded with the many variant configurations of the data clusters as shown earlier in Fig. 1, the classification process of blood cells has remained a complicated problem, especially since the cluster distributions are often complex necessitating high order nonlinear decision functions which must also contend with the ubiquitous problem of data overlap.[2,3,7,10,27]

In the process of formulating a solution, an ANN based method was considered in order to discriminate abnormal samples of patients diagnosed with acute lymphocytic leukemia from normal samples, with the highest accuracy possible.

ANNs are being successfully used for research in the medical field. For example, they have been applied to predict seizure-like event onsets,[13] to detect interictal spikes[21] and to discriminate anesthetic states,[34] to name a few. In leukemia research, they have been applied to lymphoma microarray data analysis[15,25] and to gene expression.[22,31]

The approach developed in this study is based on using NeuralStudio,[1] an ANN simulator which has been designed in support of such neural network-based applications. The approaches make use of flow cytometry parameters provided by Beckman-Coulter Corporation. In the implementation process, it is understood that subsequent to the controlled training phase, all other blood cell data provided are used as test data; and therefore all results assessed in this work reflect those of the test data.

Data Acquisition

The Beckman-Coulter data files used in this study were generated by the flow cytometer instrument,[9] which uses a light beam as well as scatter and fluorescent detectors to extrapolate information about the physical and chemical structure of the individual particles. A laser system illuminates cells and permits cell types to be quantitated and physically separated into various subpopulations. An illustration of the flow cytometer acquisition system is provided in Fig. 2.

Samples were collected at multiple hospitals and shipped to Beckman-Coulter following standard procedures. The abnormal samples were taken from a population of adult patients that have tested positive on the diseases. Normal samples were obtained at different locations. Details about subject population and data acquisition (such as instrumentation, reagents, specimen preparation, etc.) are taken into consideration in the collection process of such data.

In order to make the measurement of biological/biochemical properties of interest easier, the cells are

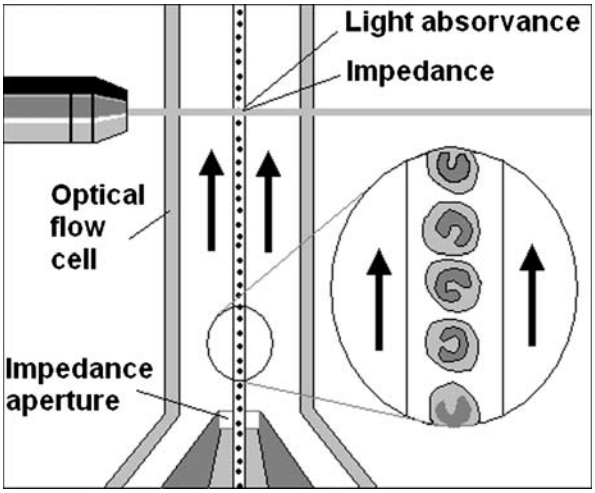

FIGURE 2. A simplified representation of the flow cytometer acquisition system (Courtesy of Beckman-Coulter Corp.).

usually stained with fluorescent dyes which bind specifically to cellular constituents. The dyes are excited by the laser beam, and emit light at longer wavelengths. Detectors pick up this emitted light, and these analog signals are converted to digital form so that they may be stored for later display and analysis. The laser increases the resolution and allows producing different wavelengths. These signals are then collected and analyzed by the optical and electronics system to extract parameters that are essential for the classification process.

The data used was extracted by the Cell Lab Quanta SC system which simultaneously measures electronic volume, side scatter and three fluorescent colors to provide excellent resolution and consequently accurate cell counting. The cytometer has multiple excitation wavelengths, including 488 nm laser and a UV light source optimized for excitation at 366, 405, and 435 nm.

Following the data acquisition process, analysis is performed to find out how many cells from the sampled population meet a criterion of interest. The output signals from the focused flow impedance and the light absorbance measurements are combined to define the white blood cell differential population clusters which were depicted earlier in Fig. 1.

Data Analysis

Each blood cell contained in a Beckman-Coulter data file is represented by 24 parameters, however, only 12 of them are directly collected using the flow cytometer, while 12 others are derived using specific log functions on the 12 principal parameters. The parameters whose suitability is investigated in this study to diagnose leukemia are DC (Direct Current Impedance), OP (Opacity), and RlsSoft (Transformed Light Scatter).

To visually appreciate flow cytometry data, 2-D dot-plots are commonly used, which show information of any combination of two parameters. Illustrative examples of dot plots using different sets of parameters are depicted in Fig. 2, which shows normal blood samples where the different cell subpopulations can be clearly identified.

However, when lymphocytes progressively accumulate in acute lymphocytic leukemia, they do not perform their functions as normal ones would, and do interfere with other blood cells. For illustration purposes, two different cases are shown in Fig. 3, where too many immature lymphocytes are highly overlapped, thus complicating the classification process.

Flow cytometry data contains usually tens of thousands of events with commonly 4–12 parameters per event. Comparison of different blood samples with such high dimensionality can be a difficult task. Therefore, a hypothesis of this study was that it is possible to simplify flow-cytometry data and still obtain satisfactory results for classification of leukemia samples.

Each blood sample provided by Beckman-Coulter is restructured in a matrix of size 8192×3, i.e., 8192 cells are in each sample with corresponding values for DC, OP, and RlsSoft. To be able to handle this type of data, any classifier would require 24576 input dimensions, which is impractical. Therefore, a reduction of dimensionality was necessary and this was achieved by feature extraction.

Extracting features from medical data can reveal hidden patterns that can be used for diagnosis as shown in Horsch *et al.*[19] and also for recognizing certain medical conditions.[6] Feature extraction is also common praxis for classification studies on leukemia as given by Foran *et al.*[17] and Sabino *et al.*[29]

In this study, the mean, peak (maximum value), standard deviation, skewness, and kurtosis of the DC, OP, and RlsSoft histograms were computed. By doing this, each blood sample could now be described by a reduced matrix of size 5×3 (5 statistical parameters * 3 data features), which was much easier to handle in term of processing requirements and for the ANN to easily converge to a solution. This feature extraction operation drastically reduced the data set size by using the most common statistical features that are related to histogram representations.

To prove the validity of the classifiers, four different case studies were conducted, namely three cases for *ALL* classification (*ALL*#1, *ALL*#2, *ALL*#3) and one for *AML* (*AML*#1). In general, two types of classifiers were created: one for *ALL* classification (3 cases) and one for *AML* (1 case). The *ALL* classification

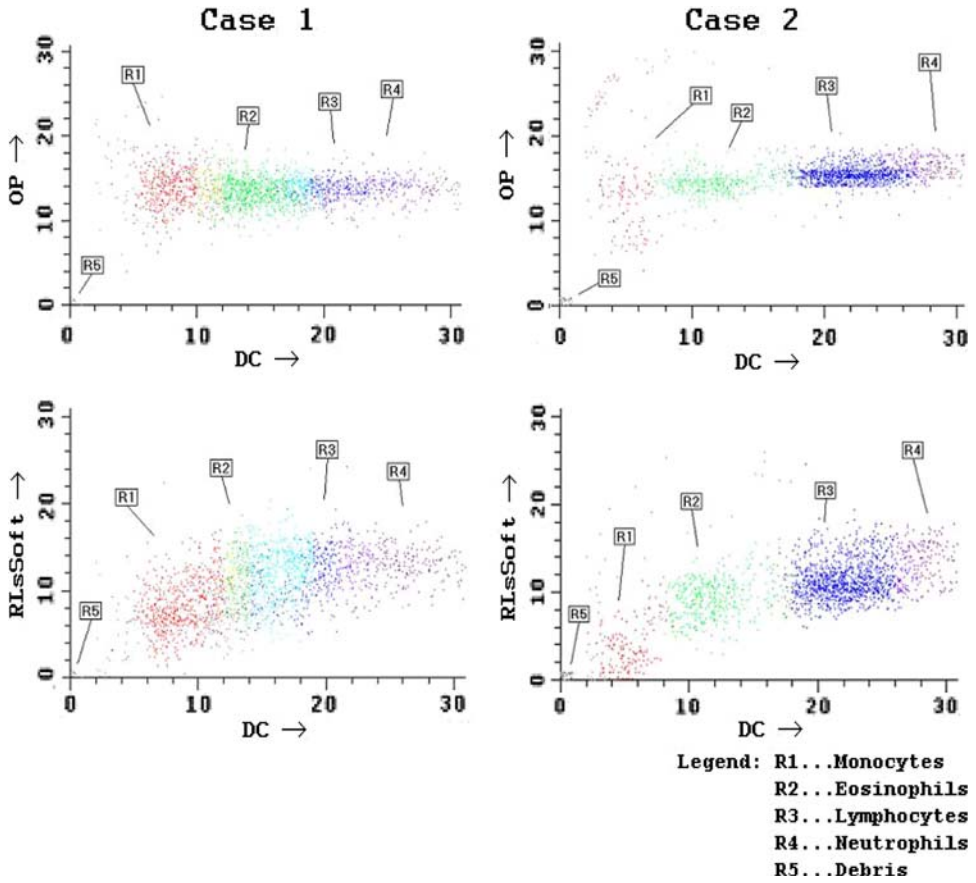

FIGURE 3. Two illustrative cases of acute lymphocytic leukemia using dot-plot displays showing extensive overlap between the different subpopulations.

algorithm was intended to classify blood samples into *ALL* or normal, whereas the *AML* classification algorithm was intended to classify blood samples into *AML* or normal.

Classification on *AML* samples was intentionally performed only once using the whole available dataset (197 samples). However, as opposed to *AML*, the *ALL* data was gradually increased in size (80, 160, and 220 samples) to produce three different data set cases. This was done in order to check if the classification results improved/deteriorated as more data were included in the analysis.

Classification Approach

Classifier Selection

The blood samples of this study contain highly overlapped cell cluster types, making linear discrimination between normal and abnormal samples not possible. However, with the use of kernels, this data can be transformed to high-dimensional spaces where linear separation can be easily achieved. Perfect candidates to deal with high-data overlap are Support Vector Machines (SVMs) and ANNs. Both are easy to model and have very simple training procedures. SVMs are a popular approach for two-category classification that is simple in use.[33] It is based on the structural risk minimization principle and focuses on finding the so-called support vectors,[14] a set of critical points that can be used to represent the decision function of the classifier. They perform classification by transforming the data into a feature space by means of kernel functions. The drawback is that SVMs depend on a limited amount of kernels. As opposed to SVMs, ANNs can be extended to multi-category classification, but more importantly, they re-create feature spaces by simply changing neuron interconnections and activation functions, and therefore, each configuration represents a different kernel.

The two 2D plots in Fig. 3 depict a high overlap of classes in the OP vs. DC plane as well as in the RLsSoft vs. DC plane. When accumulated to a 3D plane representation, this produces a complex class overlap which may not be used to train a SVM because the data is non-linear, unless a kernel is chosen which takes into account the high class overlap. But again, SVMs are not as flexible as ANNs at constructing kernels for

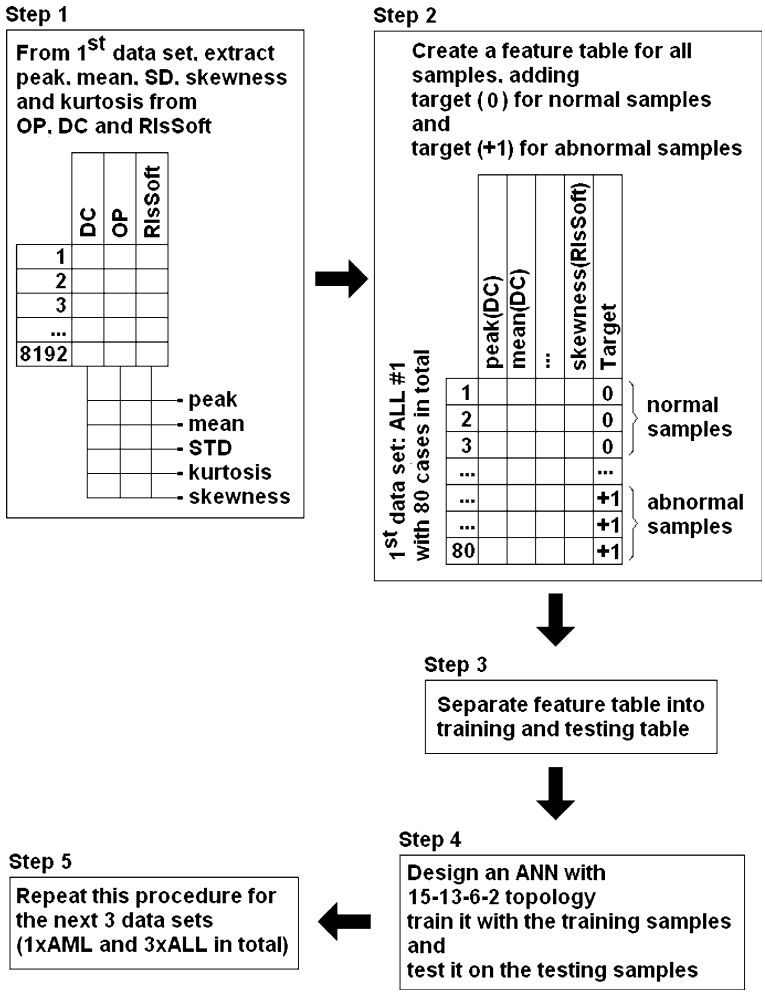

FIGURE 4. Steps implemented in the classification study.

accommodating complex class overlap. Consequently, ANNs were chosen to model the classifier.

To conduct the study, a programming tool[1] was developed at the Center for Advanced Technology and Education at Florida International University.

Classifier Design and Output Interpretation

Since classification was to be performed on entire blood samples rather than on individual cells, each blood sample was consequently represented by only 15 features, namely the peak, mean value, standard deviation, kurtosis, and skewness of each of the three parameters (DC, OP, and RlsSoft). The general structure of the steps considered for addressing this classification problem is provided in Fig. 4.

Consequently, the network architecture was designed according to the number of dimensions and type of output, i.e., 15 neurons in the input layer and 2 in the output layer to represent the classes (class 0 for normal samples and class 1 for abnormal samples). However, the output C of the binary classifier is single-valued and established as:

$$C = \underset{k}{\text{Min}} \left\| \underline{Y} - \underline{T_k} \right\| \tag{1}$$

where $\underline{Y}$ is the network output and $\underline{T_k}$ is the target vector for class k. Target vectors are $\underline{T_0} = [1, 0]$ for class 0 (normal samples) and $\underline{T_1} = [0, 1]$ for class 1 (abnormal samples). The classifier output corresponds to the class value of the winner neuron at the output layer. In this setup, a network output vector of $\underline{Y} = [y_0, y_1] = [0.2, 0.9]$ would yield a classifier output of $C = 1$ (abnormal sample), since $\|[0.2, 0.9] - [0, 1]\| < \|[0.2, 0.9] - [1, 0]\|$. Another variation having just one output neuron whose output would be from 0 (totally normal) to 1 (totally abnormal) was perfectly possible for the study, but not considered.

To generalize the practicality of such a classifier so that it can be tested on any other blood sample, it also needs to be trained on other potential diseases, which was obviously not the case of this study, as it was

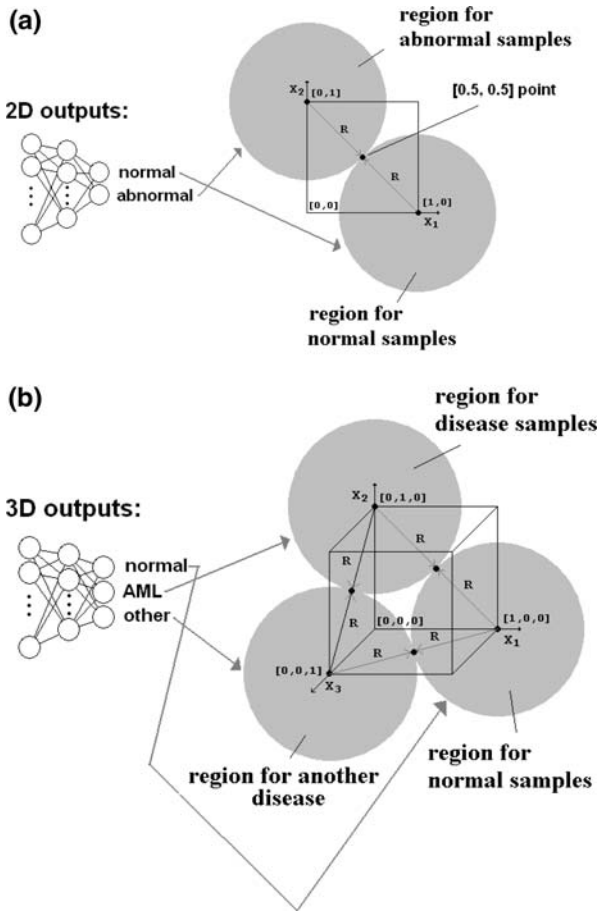

FIGURE 5. Representation of the classification threshold for (a) two-category (2D outputs) and (b) three-category (3D outputs) classifiers. The maximum classification radius *R* remains the same regardless of the number of output dimensions.

constrained to the diseases whose data was made available by Beckman-Coulter. As a consequence, a threshold measure was introduced to take into consideration the potential for samples with other diseases to exist. The [0.5, 0.5] point, which determines the maximum radius of the two circles (two classes) with no overlap, lies exactly in the middle between the two targets ([1, 0] and [0, 1]), as illustrated in Fig. 5a. Therefore, for a network output to be considered valid, the Euclidian distance between this output and any of the targets should not be greater than $0.5 * \sqrt{2}$. The $0.5 * \sqrt{2}$ threshold demarks a circular region around each of the targets [1, 0] and [0, 1] such that these regions have maximum area and do not overlap with each other. All network outputs falling inside these regions were considered valid. All other network outputs falling outside these two regions were considered undetermined. Interestingly, none of the testing points in our study yielded an undetermined outcome in our experiment.

Although this study is confined to ANN topologies with two outputs, one could expand such topologies to a higher number of outputs (>2). For example, when expanding to a 3-output ANN, target points are then established as [1, 0, 0], [0, 1, 0], and [0, 0, 1]. In the 3D-representation of Fig. 5b, the Euclidean distance between each pair of points is again $\sqrt{2}$ and half of it $\sqrt{2}/2$ can be used as a radius to draw a sphere where all outputs positioned within the sphere are expected to express a correct classification. In retrospect, such measures can serve as good classification thresholds. Therefore, any 3D network output $\underline{Y} = [y_1, y_2, y_3]$ is considered valid, when its Euclidean distance to the closest 3D target among [1, 0, 0], [0, 1, 1], and [0, 0, 1] is smaller than the set threshold. For that reason, the classifier outcome as defined in (1) is only valid when:

$$\left\| \underline{Y} - \underline{T_k} \right\| < {}^1\!/_2\sqrt{2} \tag{2}$$

where $\underline{Y} = [y_1, y_2, y_3]$ is the network output and $\underline{T_k}$ is the closest target as obtained by (1). It is believed that the ${}^1\!/_2\sqrt{2}$ threshold can be extended to any number of dimensions.

With this in mind, an assumed hypothesis is that in every well trained binary classifier, network outputs beyond the ${}^1\!/_2\sqrt{2}$ threshold can serve as evidence that a third class that was not used to train the network can be presumed. However, with the samples that were provided for this study, no network outputs were reported to fall beyond a Euclidean distance of ${}^1\!/_2\sqrt{2}$ from its closest target. It is therefore, concluded that the binary classification method used is valid, at least for the 220 samples considered.

The network topology was identical for each one of the four cases of this study. Because of the complexity of the acute leukemia data, one hidden layer was insufficient for training. Training was stopped when the cross-validation error started to increase in order to avoid network memorization. This stopping condition differed from network-to-network. Therefore, the exact moment in which the training stopped depended on the training set. We found out that the misclassification errors when the training stopped averaged less than 5% for all cases. The final topology, which is illustrated in Fig. 6, was set to 15-13-6-2 (15 inputs; two hidden layers of 13 and 6 neurons, respectively; and 2 outputs). The need for two layers is consistent with the high-data overlap. With a lesser extent of data overlap, a simpler topology would have been sufficient for the training, but such intriguing overlaps are often inherent to real-world data sets. However, in the course of this investigation, no further topologies were investigated beyond the 15-13-6-2 setup, so as to avoid running into a high number of possible topology combinations. Without major practical implications, it

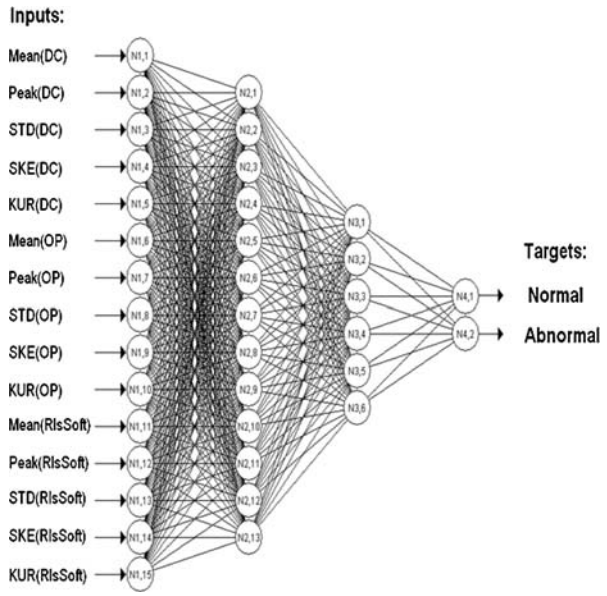

FIGURE 6. Topology of the network used for blood sample classification, showing inputs, hidden units and outputs.

can be assumed that the two hidden layers are enough to comply with the non-linearity, yielding little to no variation in the results beyond the 13 and 6 hidden neurons.

For better performance, training patterns were normalized and activation functions for the output units were chosen so as to cover the range of the targets to circumvent convergence problems, such as local minima traps, or even monotonically increasing errors. The selection and parameterization of the activation functions could be considered as the most sensible task in this study. Several trials were needed before appropriate parameters were found. Hidden units were represented by sigmoid transfer functions. For input and output units, linear activation functions were used.

Training and Testing Procedure

The training process is meant for determining optimum weights and biases that produce the best ANN topology. Prior to the training, all network weights were initialized with random values in the range $[-1, +1]$. The networks were trained with the backpropagation algorithm. In all cases, training lasted only a few minutes and was performed under cross-validation, which is a form of splitting the data available for training into two subsets: a training subset and a testing subset, such that the network is trained on the training subset and used at times for testing during training. With cross-validation, training is stopped as soon as the error of the testing subset is greater than the error of the training subset, otherwise, the trained network will memorize too much and not be able to generalize when unseen data is presented.

TABLE 1. *ALL* and *AML* cases and their partitioning into training and testing sets.

	Training	Testing	Total
ALL #1			
Normal	15 (12 pure training + 3 cross-val.)	20	35
Abnormal	15 (12 pure training + 3 cross-val.)	30	45
Total	30	50	80
ALL #2			
Normal	30 (20 pure training + 10 cross-val.)	70	100
Abnormal	30 (20 pure training + 10 cross-val.)	30	60
Total	60	100	160
ALL #3			
Normal	60 (20 pure training + 10 cross-val.)	100	160
Abnormal	30 (20 pure training + 10 cross-val.)	30	60
Total	90	130	220
AML			
Normal	60 (40 pure training + 20 cross-testing)	100	160
Abnormal	27 (18 pure training + 9 cross-testing)	10	37
Total	87	110	197

The data sets for the four cases (3 *ALL* cases and 1 *AML* case) were partitioned as shown in Table 1. The size of the cross-validation subsets was selected in accordance to the number of normal and abnormal samples in each case. The size of each testing set was set to 1.6–1.8 times the size of the corresponding training set. As shown in Table 1, in case *ALL* #1, cross-validation was performed at a 1/5 ratio (cross-testing to pure training), whereas in the remaining cases, the cross-validation ratio was set to 1/3.

The results provided in the following section are based on the average classifier that was obtained after averaging the classifier weights obtained in five training trials.

RESULTS AND DISCUSSION

Classifying Acute Lymphocytic Leukemia (ALL) Samples

Classification performance was evaluated by means of Receiver Operating Characteristics (ROC) analysis[20,30] which contains information about actual and predicted categories as obtained by a classification system. Since the *ALL* data was received in a sequential way increasing from 50 to 130 samples, three different classifiers were established with incremental amounts of samples received (50, 100, and 130). It is noted that this performance increased in terms of classification accuracy with increased data size. This fact is depicted in Fig. 7 where an ascending trend is noted for the TP fraction or sensitivity varying from 80% (with 50 samples) up to 96.67% (with the entire

130 samples), and a descending trend is observed for the FP rate from 10% (with 50 samples) to 1% (with the entire 130 samples). The results of the *ALL* sample classifiers are illustrated in Tables 2 and 3.

Classifying Acute Myeloid Leukemia Samples (AML samples)

In a supplementary application, a similar ANN topology (15-13-6-2) was used as a starting platform to train a different classifier for the corresponding *AML* dataset.

For this part of the study, 197 samples were available, whereas data partitioning was set to 60 normal and 27 abnormal samples (refer back to Table 1). Training was stopped after a 3.23% training set error and a 0.00% cross-validated testing set error was obtained. Testing was then performed on the remaining 110 samples (100 normal and 10 abnormal), which were previously excluded from training.

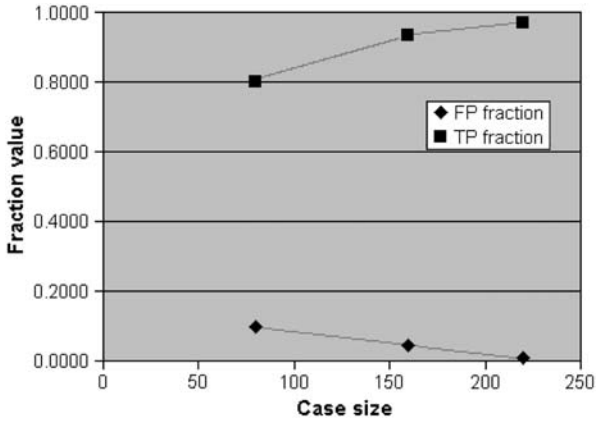

FIGURE 7. Trends of the TP and FP fraction values vs. increasing data size for the *ALL* cases.

TABLE 2. *ALL* and *AML* testing results.

	TP	FP	FN	TN
ALL #1	24	2	6	18
ALL #2	28	3	2	67
ALL #3	29	1	1	99
AML	9	2	1	98

To compare with the results of the *ALL* sample classifier implementation, the results of the *AML* sample classifier are illustrated in Tables 2 and 3. In total, 96 of the 100 normal samples were correctly classified and among the 10 *AML* samples, only one sample was misclassified as normal. The performance of this sample classifier was remarkably high at 90% for the TP fraction and 2% for the FP fraction.

CONCLUSION

This study addressed a critical classification problem that accurately delineated clusters of normal blood samples from clusters of blood samples with acute leukemia. The main objective was to provide a classifier for leukemia blood samples that performs well on a reduced amount of flow-cytometry parameters. As a result, an integrated software platform was developed that would serve as a reference tool for diagnostic references in flow cytometry.[32] As far as competing methods, most consist of rule-based, expert system and type classifiers including cell images, simple peripheral blood samples, and gene expression, and not ANN as was implemented in this study.[16,18,26] Furthermore the proposed classifiers can also be used as supporting tools in the diagnosis of theses diseases.

Classifiers were tested on the samples that were suspected to have one of the two specific diseases, but in general, any blood sample suspected of *ALL* or *AML* would need to be tested on the two different classifiers, whereas the final decision will correspond to the highest classifier or network output. In pattern classification, it is perfectly valid to present patterns to different binary classifiers, such as the one-vs.-all algorithm[12,27,28] especially when the subject can have different disease states.

It is also important to emphasize that in classification studies, increasing the size of the population does not necessarily lead to better results. This is more evident when data are contaminated with high class overlap. For that reason, it can be considered a significant outcome of this investigation that the classification results improved as more *ALL* data were

TABLE 3. Performance results for the *ALL* and *AML* samples.

Leukemia type	Total training data (Normal/Abnormal)	Total testing data (Normal/Abnormal)	TP fraction (%)	FP fraction (%)	Accuracy (%)
ALL	30 (15/15)	50 (20/30)	80.00	10.00	84.04
	60 (30/30)	100 (70/30)	93.33	4.29	95.00
	90 (60/30)	130 (100/30)	96.67	1.00	98.46
AML	87 (60/27)	110 (100/10)	90.00	2.00	97.27

included in the analysis. All classification results are summarized in Table 3.

The main contributions can then be summarized as follows:

- Proof that it is possible to train ANNs to classify blood samples suspected of *ALL* or *AML* by using a reduced amount of parameters that are obtained from flow cytometry.
- Developed a method to ensure that the ANN architecture is optimally configured yielding the best possible results under the complexity of this multidimensional problem.
- Ensured through the generalized approach that has been considered, that any other form of histogrammed data could be automatically entered such that analysis and classification can extend to other disease states beyond the diseases treated in this study.

In retrospect, improvement of the TP fraction above 95% for the *ALL* cases is viewed as significant and is presented in this study as an interesting outcome which should be considered in an optimized application case for flow-cytometry data.[4]

ACKNOWLEDGMENTS

The authors appreciate the support provided by the National Science Foundation under Grants CNS-0426125, HRD-0833093, CNS-0520811, CNS-0540592. The authors are grateful for the clinical support provided through the Ware Foundation and the joint Neuro-Engineering Program with Miami Children's Hospital. We also thank Beckman-Coulter Corporation for providing us the flow-cytometry data, which was critical for this research.

REFERENCES

[1]Adjouadi, M., and M. Ayala. Introducing neural studio: an artificial neural networks simulator for educational purposes. *Comput. Educ. J.* 14(3):33–40, 2004.

[2]Adjouadi, M., and N. Fernandez. An orientation-independent imaging technique for the classification of blood cells. *J. Part. Part. Syst. Charact.* 18(2):91–98, 2001.

[3]Adjouadi, M., C. Reyes, J. Riley, and P. Vidal. Adaptive filtering for flow-cytometric particles. *J. Part. Part. Syst. Charact.* 17(3):126–133, 2000.

[4]Adjouadi, M., C. Reyes, P. Vidal, and A. Barreto. An analytical approach to signal reconstruction using Gaussian approximations applied to randomly generated data and flow cytometric data. *IEEE Trans. Signal Process.* 48(10):2839–2849, 2000.

[5]Adjouadi, M., N. Zong, and M. Ayala. Multidimensional pattern recognition and classification of white blood cells using support vector machines. *Part. Part. Syst. Charact.* 22:107–118, 2005.

[6]Ahlstrom, C., P. Hult, P. Rask, *et al.* Feature extraction for systolic heart murmur classification. *Ann. Biomed. Eng.* 34(11):1666–1677, 2006.

[7]Albitar, M., T. Manshouri, Y. Shen, *et al.* Myelodysplastic syndrome is not merely "preleukemia". *Blood* 100(3):791–798, 2002.

[8]Beckman-Coulter Corp., FL. AcV Differential and Case Studies, Monograph. Available: http://www.beckmancoulter.com/literature/ClinDiag/AcT5diffCaseStudies.pdf, Bulletin 9151, 2000.

[9]Beckman Coulter Cytometry Equipment. Online: http://www.coulter.com/products/Discipline/Life_Science_Research/pr_disc_flow_cytometry.asp?bhcp=1, December 2006.

[10]Bohnke, A., F. Westphal, A. Schmidt, R. A. El-Awady, and J. Dahm-Daphi. Role of p53 mutations, protein function and DNA damage for the radiosensitivity of human tumour cells. *Int. J. Radiat. Biol.* 80(1):53–63, 2004.

[11]Buño, I., W. A. Wyatt, A. R. Zinsmeister, J. Dietz-Band, and R. T. Silver. A special fluorescent in situ hybridization technique to study peripheral blood and assess the effectiveness of interferon therapy in chronic myeloid leukemia. *Blood* 92(7):2315–2321, 1998.

[12]Burges, C. J. C. A tutorial on support vector machines for pattern recognition. *Data Min. Knowl. Disc.* 2(2):121–167, 1998.

[13]Chiu, A. W. L., E. E. Kang, M. Derchansky, *et al.* Online prediction of onsets of seizure-like events in hippocampal neural networks using wavelet artificial neural networks. *Ann. Biomed. Eng.* 34(2):282–294, 2006.

[14]Cristianini, N., and J. Shawe-Taylor. An Introduction to support vector machines and other kernel-based learning methods. New York: Cambridge University Press, 2000.

[15]De Paz, J. F., S. Rodríguez, J. Bajo, and J. M. Corchado. Case-based reasoning as a decision support system for cancer diagnosis: a case study. *Int. J. Hybrid Intell. Syst.* 6(2):97–110, 2009.

[16]Feki, S., H. El Omri, M. A. Laatiri, S. Ennabli, K. Boukef, and F. Jenhani. Contribution of flow cytometry to acute leukemia classification in Tunisia. *Dis. Markers* 16(3–4):131–133, 2000.

[17]Foran, D. J., D. Dorin Comaniciu, P. Meer, and L. A. Goodell. Computer-assisted discrimination among malignant lymphomas and leukemia using immunophenotyping, intelligent image repositories, and telemicroscopy. *IEEE Trans. Inform. Technol. Biomed.* 4(4):265–273, 2000.

[18]Haferlach, T., A. Kohlmann, S. Schnittger, M. Dugas, W. Hiddemann, W. Kern, and C. Schoch. Global approach to the diagnosis of leukemia using gene expression profiling. *Blood* 106(4):1189–1198, 2005.

[19]Horsch, K., M. L. Giger, L. A. Venta, and C. J. Vyborny. Computerized diagnosis of breast lesions on ultrasound. *Med. Phys.* 29(2):157–164, 2002.

[20]Kohavi, R., and F. Provost. Glossary of terms. *Mach. Learn.* 30:271–274, 1998.

[21]Kurth, C., F. Gillam, and B. J. Steinhoff. EEG spike detection with a Kohonen feature map. *Ann. Biomed. Eng.* 28(11):1362–1369, 2000.

[22]Liu, B., Q. Cui, T. Jiang, and S. Ma. A combinational feature selection and ensemble neural network method for classification of gene expression data. *BMC Bioinform.* 5:136, 2004. doi:10.1186/1471-2105-5-136.

[23]Lopes Ferrari, M., J. S. Rodrigues Oliveira, M. Romeo, and J. Kerbauy. Fluorescent in situ hybridization (FISH)

for BCR/ABL in chronic myeloid leukemia after bone marrow transplantation. *Sao Paulo Med. J./Rev. Paul Med.* 119(1):8–16, 2001.

[24]Mark, H. F., W. Sikov, H. Safran, T. C. King, and R. C. Griffith. Fluorescent in situ hybridization for assessing the proportion of cells with trisomy 4 in a patient with acute non-lymphoblastic leukemia. *Ann. Clin. Lab. Sci.* 25(4):330–335, 1995.

[25]O'Neill, M. C., and L. Song. Neural network analysis of lymphoma microarray data: prognosis and diagnosis near-perfect. *BMC Bioinform.* 4:13, 2003. doi:10.1186/1471-2105-4-13.

[26]Prasad, B., and W. Badawy. High-throughput identification and classification algorithm for leukemia population statistics. *J. Imaging Sci. Technol.* 52(3):030509.1–030509.23, 2008.

[27]Reyes, C., and M. Adjouadi. A directional clustering technique for random data classification. *J. Cytometry* 27(2):126–135, 1997.

[28]Rifkin, R., and A. Klautau. In defense of one-vs-all classification. *J. Mach. Learn. Res.* 5:101–141, 2004.

[29]Sabino, D. M. U., Ld. F. Costa, E. G. Rizzatti, and M. A. Zago. A texture approach to leukocyte recognition. *Imaging Bioinform. III* 10(4):205–216, 2004.

[30]Tilbury, J., P. Eetvelt, J. Garibaldi, J. Curnow, and E. Ifeachor. Receiver operating characteristic analysis for intelligent medical systems—a new approach for finding confidence intervals. *IEEE Trans. Biomed. Eng.* 47(7):952–963, 2000.

[31]Tung, W., and C. Quek. GenSo-FDSS: a neural-fuzzy decision support system for pediatric ALL cancer subtype identification using gene expression data. *Artif. Intell. Med.* 33(1):61–88, 2004.

[32]University of Leicester, Department of Microbiology & Immunology, Cells of the Blood. www.micro.msb.le.ac.uk/MBChB/bloodmap.

[33]Vapnik, V. N. The Ature of Statistical Learning Theory. New York: Springer, 1995.

[34]Zhang, X. S., R. J. Roy, D. Schwender, *et al.* Discrimination of anesthetic states using mid-latency auditory evoked potential and artificial neural networks. *Ann. Biomed. Eng.* 29(5):446–453, 2001.